

## Research Article

David J. Unger\*

# Visualizing the crack driving force through fluid analogy

<https://doi.org/10.1515/jmbm-2019-0011>

Received Aug 27, 2019; accepted Nov 01, 2019

**Abstract:** It is shown that the crack driving force for a fundamental antiplane crack problem is analogous to the limiting case of the force acting on an ideal fluid on free streamlines that form at the ends of flow around two parallel plates.

**Keywords:** Riabouchinsky free streamline problem, J integral

## 1 Introduction

One of the more difficult concepts for students to comprehend in an introductory course on fracture mechanics is the crack driving force. By employing a simple hydrodynamic analogy between the free streamline problem for potential flow around two finite-length plates [1, 2] and an analogous mode III slot problem [3–6], visualization of an analogous force acting on the free streamlines is possible. Recovery of the standard crack driving force for a linear elastic mode III crack problem can be obtained from the mode III slot solution by allowing the width of the slot to mathematically approach zero.

In Figure 1a, one finds a schematic drawing of a mode III slot problem as analyzed previously in [6]. Because of the symmetry of the problem with respect to the vertical axis  $C'B'BC$ , only the right hand side of the infinite plate is depicted. Similarly, in Figure 1b, the analogous free streamline problem of [1, 2] is depicted.

The slot geometry is designated by the letters  $B'A'MAB$  in Figure 1a. The stationary fluid boundary has an identical labeling in Figure 1b, and is composed of the two-dimensional plates  $A'B'$  and  $AB$  plus the free streamline  $A'MA$ .

In the slot problem a remote antiplane shear traction is designated in the figure by  $\tau_\infty$ ; whereas, in the fluid flow problem the uniform velocity at infinity is labeled  $v_\infty$ .

The slot boundary is traction free along its surface  $B'A'MAB$ . The basic tenets along any free streamline are that the pressure and speed are constant [2]. A fluid streamline follows the path  $C'B'A'MABC$  around the plates where at the ends of the plates a free streamline forms. Along the free streamline  $A'MA$ , a velocity discontinuity  $\Delta v$  occurs separating the moving fluid from the stationary fluid.

In cases when the moving fluid is liquid water, the stationary fluid can be interpreted as water vapor thus defining a class of problems associated with cavitation phenomena [2].

The shape of the end of the slot  $A'MA$  and also of the free streamline are given in Cartesian coordinates  $(x_R, y_R)$  by the following parametric relationships in  $\theta$

$$\begin{aligned} x_R &= -(a/2) [-(1-k') \cos \theta + k'K(m) - E(m)], \quad (1) \\ y_R &= (a/2)(1+k') \left[ E \left( \sin^{-1} \left( \frac{\sin \theta}{k_1} \right), k_1^2 \right) \right. \\ &\quad \left. - \frac{(1-k')^2}{(1+k')^2} F \left( \sin^{-1} \left( \frac{\sin \theta}{k_1} \right), k_1^2 \right) \right], \\ &\text{for } -\pi/2 \leq \theta \leq \pi/2, \end{aligned}$$

where  $a$  is a scaling parameter with units of length. The specific definitions of the elliptic integrals in (1) are those adopted in [7].

The various relationships among parameters appearing in the elliptic integrals of (1) are

$$m = 1 - m_1, k' = \sqrt{m_1}, k_1 = \frac{2\sqrt{k'}}{1+k'}, 0 \leq m_1 \leq 1. \quad (2)$$

The Cartesian coordinates of two key points  $A$  and  $M$ , shown in the figures, are respectively

$$\begin{aligned} x_A &= \frac{a}{2} \left[ -\sqrt{m_1}K(m) + E(m) + \frac{(1-\sqrt{m_1})^2}{1+\sqrt{m_1}} \right], \quad (3) \\ y_A &= a [E(m_1) - (1-\sqrt{m_1})K(m_1)]. \end{aligned}$$

$$\begin{aligned} x_M &= \frac{a}{2} [-\sqrt{m_1}(K(m)+1) + E(m)+1], \quad (4) \\ y_M &= 0. \end{aligned}$$

\*Corresponding Author: David J. Unger: Department of Mechanical and Civil Engineering University of Evansville, Evansville, IN 47722, United States of America; Email: du2@evansville.edu

As  $m_1 \rightarrow 0$ , both  $x_A$  and  $x_M \rightarrow a$ , and  $y_A \rightarrow 0$ . Therefore a crack problem of crack length  $2a$  can be recovered from the slot problem as a limiting case as  $m_1 \rightarrow 0$ .

Note the Figures 1 were generated with a value of  $m_1 = 0.01$  and  $a = 1$ .

## 2 Fluid flow analysis

Let us follow a streamline  $C'B'A'MABC$  beginning at the bottom of Figure 1b where  $y$  is at negative infinity. For convenience, it is assumed the pressure  $p_\infty$  there is zero and the speed has the arbitrary value  $v_\infty$ .

Bernoulli's equation has the general form along a streamline

$$p + \frac{1}{2}\rho v^2 = \text{const}, \quad (5)$$

where  $\rho$  (constant) is the density of an incompressible, inviscid fluid. Using the values of pressure and velocity at infinity, one finds that the value of the *const* in (5) is

$$\text{const} = \frac{1}{2}\rho v_\infty^2. \quad (6)$$

At the start of the free streamline  $A'$  and continuing to  $A$  one finds from (5) and (6) that

$$p_c + \frac{1}{2}\rho c^2 = \frac{1}{2}\rho v_\infty^2, \quad (7)$$

where  $p_c$  is the pressure of the moving fluid and  $c$  is its speed along the free streamline. Along the interface of the free streamline and the stationary fluid, Newton's third law requires that the pressures be opposite in direction as they act on this fluid membrane separating the media. Therefore the pressure of the stationary fluid  $p_c$  in the cavity needed to counterbalance the pressure of the moving fluid is

$$p_c = \frac{1}{2}\rho (c^2 - v_\infty^2). \quad (8)$$

Now the differential driving force per unit thickness that (8) induces along the free streamline is

$$dF_D = p_c \cos \alpha ds \quad (9)$$

where  $\alpha$  is the angle to a unit normal to the boundary  $A'MA$  as shown in Figure 1a, and  $ds$  is the differential arc length along the free streamline. Geometrically, the following differential relationship exists along  $A'MA$

$$dy = \cos \alpha ds. \quad (10)$$

Consequently by substituting (8) and (10) into (9) one finds

$$\begin{aligned} F_D &= \frac{1}{2}\rho (c^2 - v_\infty^2) \int_{-y_A}^{y_A} dy \\ &= \rho (c^2 - v_\infty^2) y_A, \end{aligned} \quad (11)$$

where  $y_A$  is given by the second equation in (3). Now by an analogy found previously in [6]

$$k' = \left(\frac{v_\infty}{c}\right)^2 \quad (12)$$

and using (2), the form of (11) becomes

$$F_D = \rho v_\infty^2 \left(\frac{1}{\sqrt{m_1}} - 1\right) y_A. \quad (13)$$

For use in comparing the fluid problem to the slot problem, the distance separating the two surfaces  $A'B'$  and  $AB$  will be small, and correspondingly the value of  $1/\sqrt{m_1}$  will be large. Under these circumstances, the second term in the parentheses of (13) may be neglected to yield the approximation

$$F_D = \rho v_\infty^2 \frac{y_A}{\sqrt{m_1}}. \quad (14)$$

## 3 Slot analysis

One of the more interesting features of the slot solution of [6] is that the equivalent shear stress is constant along the rounded slot tips. The equivalent shear stress is defined as

$$\tau_{eq} = \sqrt{\tau_{xz}^2 + \tau_{yz}^2}, \quad (15)$$

where  $\tau_{xz}$  and  $\tau_{yz}$  are the antiplane shear stresses. By identifying  $\tau_{eq}$  as the yield strength in pure shear  $\tau_0$ , the von Mises or Tresca yield condition is satisfied on the rounded ends of the slot. This characteristic allows the solution to be interpreted as being associated with either a purely linear elastic problem or as a linear elastic problem with incipient plastic material at the slot ends.

The crack driving force for linear elastic fracture mechanics is often designated by  $\mathcal{G}$  in honor of A. A. Griffith [8]. For linear elastic fracture mechanics the energy release rate may be calculated from the  $J$ -integral [9]. The  $J$ -integral for the slot problem in this analysis reduces to

$$J = \int_{-y_A}^{y_A} W dy, \quad (16)$$

as there are no tractions along the slot surface. The symbol  $W$  in (16) represents the strain energy density. For linear elastic materials, the  $J$ -integral is equal to  $\mathcal{G}$  and consequently the crack driving force.

Along the slot tip, the strain energy density may be calculated from the relationship

$$W = \frac{1}{2G} (\tau_{xz}^2 + \tau_{yz}^2) = \frac{\tau_0^2}{2G}, \quad (17)$$

where  $G$  is the shear modulus, and  $\tau_0$  is the constant state of equivalent stress along the slot tip. In [6] it was determined that

$$\tau_0 = \tau_\infty / \sqrt{k'} = \tau_\infty / m_1^{1/4}, \quad (18)$$

which is the solids counterpart to fluids relationship (12) for the slot problem.

Therefore, by substituting (17) and (18) into (16), one obtains

$$J = \frac{\tau_0^2}{G} y_A = \frac{\tau_\infty^2}{G} \frac{y_A}{\sqrt{m_1}}. \quad (19)$$

If one compares (19) to (14), the analogy between the two problems is obvious.

By taking the limit of (19) as  $m_1 \rightarrow 0$  the crack driving force of the mode III crack problem is recovered

$$\lim_{m_1 \rightarrow 0} J = \frac{\tau_\infty^2 \pi a}{2G}. \quad (20)$$

Similarly, the limit of either (13) or its approximation (14) is

$$\lim_{m_1 \rightarrow 0} F_D = \frac{\rho v_\infty^2 \pi a}{2}. \quad (21)$$

Naturally the visual impact of forces acting on a surface associated with (21) is lost as sides  $A'B'$  and  $AB$  approach one another and the surface  $A'MA$  degenerates to a point.

## 4 Closing

Hopefully, this analysis can serve in the classroom as an aid to visualizing the crack driving force through fluid analogy.

It should be mentioned that the results presented here are not directly applicable to modes I and II crack problems as the governing partial differential equation is different from that of the mode III problem. For plane problems the governing partial differential equation is biharmonic. Both mode III crack problems and ideal fluid flow problems are governed by Laplace's equation. In addition, there is no known analogy to the free streamline solution for the biharmonic equation.

It is also worth noting that the approximate mode I and mode II slot problem solutions proposed in [3, 4], for the same slot geometry analyzed here for the mode III slot problem, have been shown in later years to be invalid. However, a good approximation for the stress concentration factor of the mode I slot problem of this type does exist [5]. This approximate stress concentration factor was verified using the commercial finite element program Ansys® 14.5, (Ansys, Inc., Canonsburg, PA, USA).

## References

- [1] Riabouchinsky D., On steady fluid motions with free surfaces, Proc. Lond. Math. Soc. (2), 1921, 19(1), 206-215.
- [2] Milne-Thomson L.M., Theoretical Hydrodynamics, 5th ed., 1996, Dover, Mineola.
- [3] Unger D.J., Linear elastic solutions for slotted plates, J. Elasticity 2012, 108(1), 67-82.
- [4] Unger D.J., Erratum to: Linear elastic solutions for slotted plates, J. Elasticity, 2012, 108(1), 83.
- [5] Unger D.J., Linear elastic solutions for slotted plates revisited, Proceedings 24th Int. Congr. Theor. Appl. Mech., ed. JM Floryan, ICTAM, Montreal, 2017, 2042-2043.
- [6] Unger D.J., Free streamline hydrodynamic analogy for a linear elastic antiplane slot problem with perfectly plastic ligaments at its ends, J. Elasticity 2018, 132(2), 261-270.
- [7] Abramowitz M., Stegun I.A., Handbook of Mathematical Functions with Formulas, Graphs and Mathematical Tables. National Bureau of Standards, Series 55, U.S. Printing Office, Washington, DC, 1964.
- [8] Hellen K., Introduction to Fracture Mechanics, 1984, 52, McGraw-Hill, New York.
- [9] Rice J.R., A path independent integral and approximate analysis of strain concentrations by notches and cracks, J. Appl. Mech., 1968, 35(2), 379-386.

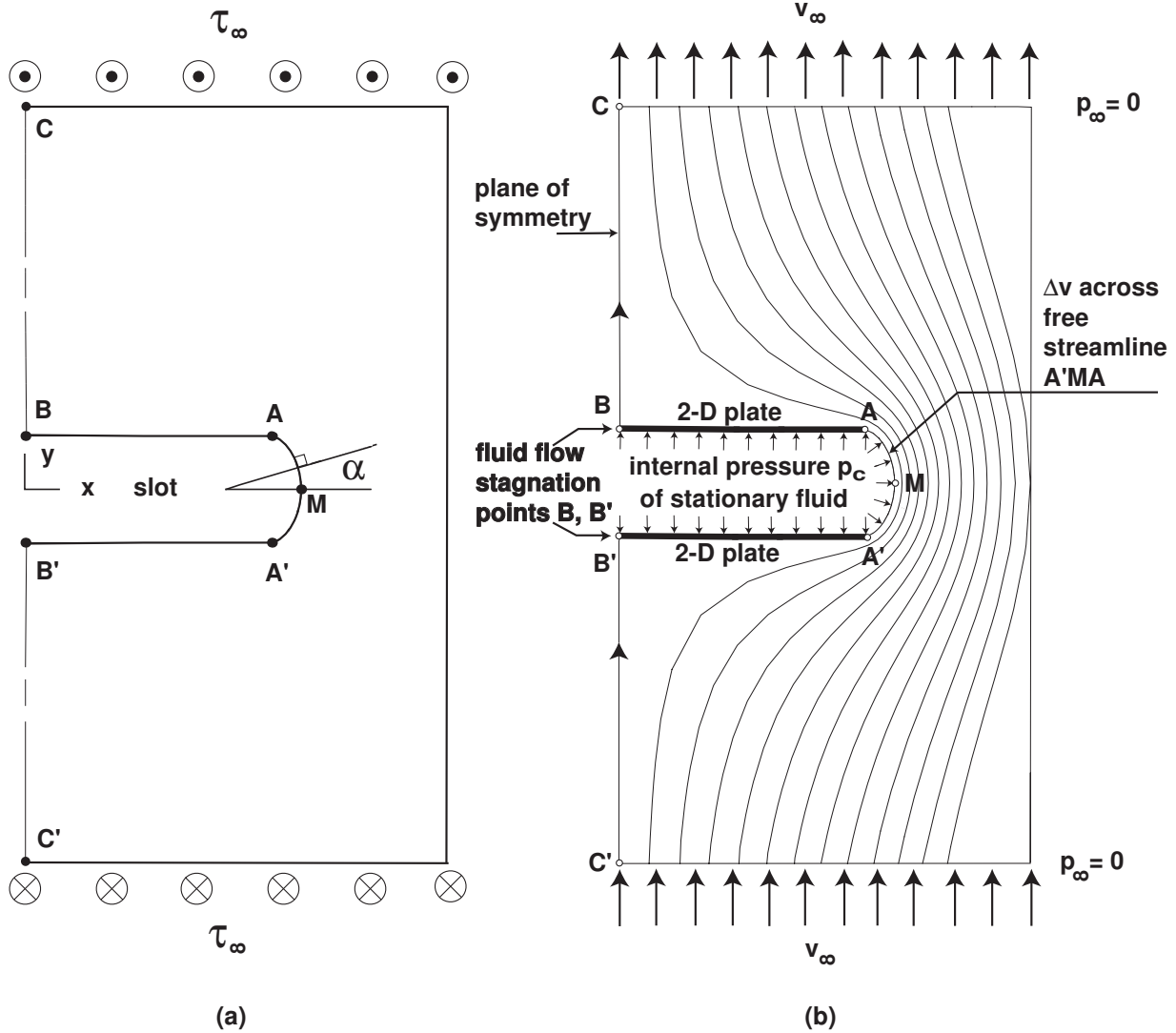


Figure 1: a) Mode III slot problem b) Free streamline problem around two plates

## Appendix A

### Elliptic integrals

The incomplete elliptic integrals of the first and second kinds that are used in (1) are defined respectively as

$$\left. \begin{aligned} F(\phi, m) &= \int_0^\phi \frac{d\theta}{\sqrt{1 - m\sin^2\theta}} \\ E(\phi, m) &= \int_0^\phi \sqrt{1 - m\sin^2\theta} d\theta \end{aligned} \right\} 0 \leq m \leq 1. \quad (A1)$$

For  $\phi = \pi/2$  these functions (A1) are called complete elliptic integrals of the first and second kind respectively and

are designated by

$$F(\pi/2, m) = K(m), \quad E(\pi/2, m) = E(m). \quad (A2)$$

## Appendix B

### Plotting streamlines

In order to plot the streamlines shown in Figure 1b, one defines the following complex variable  $\zeta$

$$\zeta = \xi + i\eta, \quad (A3)$$

where  $\xi$  and  $\eta$  are real variables. A particular streamline is represented in the figure by a constant value of  $\xi$ . Similarly, a constant value of  $\eta$  represents an ideal fluid poten-

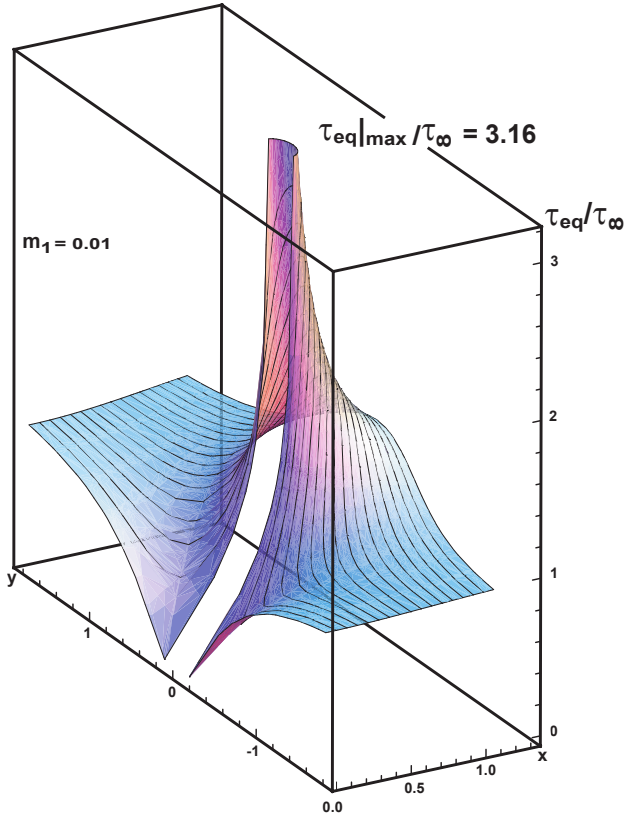


**Figure 2:** Equivalent shear stress magnitude and trajectory lines

tial line, which is orthogonal to the family of streamlines (potential lines are not shown in Figure 1b).

Next, a complex representation  $z = x + iy$  of the physical plane in Cartesian coordinates  $(x, y)$  is defined [3, 4] as

$$z = a \left\{ k' w - E(\phi, m) + \frac{dn(w, m)}{1+k'} [k' sc(w, m) - cs(w, m)] \right\}, \quad (A4)$$

where  $\phi$  is expressed in terms of the Jacobian elliptic amplitude [7] as

$$\phi = \text{amp}(w, m), \quad (A5)$$

and the function  $w = w(\zeta)$  in (A4) and (A5) is given by

$$w = sc^{-1} \left( b \left( -\zeta + \sqrt{\zeta^2 + 4d} \right), m \right). \quad (A6)$$

The parameter  $a$  of (A4) is the same as in (1). The parameters  $b$  and  $d$  of (A6) are defined in terms of those previously defined in (2) by the following relationships

$$b = \frac{1}{2} \left( 1 + \frac{1}{k'} \right), \quad d = \frac{k'}{(1+k')^2}. \quad (A7)$$

The functions  $sc$  and  $cs$  in (A4) are Jacobian elliptic amplitude functions [7] and  $sc^{-1}$  is the inverse function of  $sc$  in (A6).

The Jacobian elliptic amplitude  $\text{amp}(w, m)$  is defined as the inverse function of the complete elliptic integral of the first kind.

Figure 1b was generated using the following limits

$$0 \leq \xi \leq 1, \quad -2 \leq \eta \leq 2, \quad (A8)$$

with the parameter  $m_1 = 0.01$ . Note that (A4) was defined in [3, 4] for the half plane  $-\infty \leq x \leq 0$ , so that Figure 1b was actually generated as the reflection of the left-hand half plane across the  $y$ -axis using this relationship.

## Appendix C

### Equivalent shear stress trajectory lines

An analogy exists between the streamlines shown in Figure 1b and the equivalent shear stress trajectory lines of the slot problem.

In Figure 2, the equivalent shear stress trajectory lines are shown where a Westergaard stress function was used [3, 4] to determine the equivalent shear stress (15)

$$Z_{III} = \tau_{\infty} nd(w, m), \quad \text{where} \quad (A9)$$

$$\tau_{xz} = \text{Im}(Z_{III}), \quad \tau_{yz} = \text{Re}(Z_{III}).$$

The function  $nd$  in (A9) is the reciprocal of the Jacobian elliptic amplitude function  $dn$ . The equivalent shear stress (15) is everywhere tangent to its trajectory lines. The equivalent shear stress trajectory lines shown in Figure 2 are identical mathematically to those relationships used for plotting the streamlines shown in Figure 1b. Along the slot tip a maximum equivalent shear stress is depicted in Figure 2 for  $m_1 = 0.01$ . This value is analogous to the maximum speed  $c$  of (12) found along the free streamline in the fluid flow problem. Both the maximum equivalent shear stress along the slot tip and the maximum speed along the free streamlines remain constant along curves  $AMA'$  of Figures 1.

## Appendix D

### Reduction of slot geometry to crack line

An alternative orthogonal coordinate system to (A4) for the slot problem was provided in [5, 6] as

$$z = \frac{a}{2} \left\{ -(1 - k') \frac{1 + \zeta^2}{2\zeta} + \operatorname{sgn}(\operatorname{Re}\zeta) [k' K(m) - E(m)] + i(1 + k') \left[ E \left( \sin^{-1} \frac{i}{k_1} \frac{1 - \zeta^2}{2\zeta}, k_1^2 \right) - \frac{(1 - k')^2}{(1 + k')^2} F \left( \sin^{-1} \frac{i}{k_1} \frac{1 - \zeta^2}{2\zeta}, k_1^2 \right) \right] \right\}, \quad (\text{A10})$$

where the various elliptic integral parameters are the same as in (2) and  $a$  is the same scaling factor as in (1).

If one substitutes

$$\zeta = \exp(-u + iv), \quad (\text{A11})$$

into (A10), then elliptical coordinates are obtained as a limiting case as  $m_1 \rightarrow 0$

$$z = a \cosh(u + iv). \quad (\text{A12})$$

In (A12)  $u$  is a family of confocal ellipses and  $v$  is a family of hyperbolas orthogonal to the ellipses. The range of the elliptical coordinates in (A12) are  $0 \leq u \leq \infty$ ,  $-\pi \leq v \leq \pi$ . The slot for  $m_1 = 0$  reduces to the elliptic coordinate  $u = 0$ , which represents a slit in the plane spanning  $-a \leq x \leq a$ ,  $y = 0$ . Consequently, points  $AMA'$  in Figure 1a coalesce to a single point at  $x = a$ .